Washout control of a cyclic vehicular traffic flow

著者	Yamamoto Shigeru, Sakaguchi Eiji
journal or publication title	IFAC Proceedings Volumes (IFAC-PapersOnline)
volume	18
number	Part 1
page range	8421-8426
year	2011-01-01
URL	http://hdl.handle.net/2297/35642

doi: 10.3182/20110828-6-IT-1002.02388

Washout Control of a Cyclic Vehicular Traffic Flow

Shigeru Yamamoto * **Eiji Sakaguchi** **

* *Faculty of Electrical and Computer Engineering, Institute of Science and Engineering, Kanazawa University, Japan (Tel : +81-76-234-4849; e-mail: shigeru@t.kanazawa-u.ac.jp).*
** *Division of Electrical and Computer Engineering, Graduate School of Natural Science and Technology, Kanazawa University, Japan (e-mail: sakaguchi@moccos.ec.t.kanazawa-u.ac.jp).*

Abstract: In this paper, we consider a decentralized control problem for suppressing the traffic jam in a cyclic traffic flow. In recent years, to explain the mechanism that causes the traffic jam, several experiments have been done for multiple vehicles on the circle. The traffic jam can be explained by the so-called optimal velocity model, the optimal velocity function which is a nonlinear function of the headway of the preceding vehicle and describes driver's characteristics. In this paper, we apply washout control to suppress the traffic jam in a cyclic traffic flow not to disturb driver's characteristics. Then, we show a method to select parameters to keep stability of the closed-loop system. We find that our proposed method for selecting parameters is better than the conservative method using the small gain theorem. In addition, we illustrate the effectiveness with several simulations.

Keywords: traffic flow, optimal velocity model, decentralized control, washout control, formation.

1. INTRODUCTION

The traffic jam daily occurs which yields a loss by increasing traffic-transportation time and it makes driver exhausting. Hence, control systems which can track following vehicle's velocity rapidly are required for suppressing the traffic jam. By using such control systems, we expect to achieve not only smooth traffic flow but also energy-saving and support driver.

It is shown that a washout control method (Takimoto, Yamamoto, and Oku (2008)) can suppress the traffic jam phenomenon in the unidirectional optimal velocity model (Yamamoto and Sakaguchi (2009)). On the other hand, to explain the mechanisms that cause the traffic jam, experiments have been run multiple vehicles on the circle (Sugiyama *et al.* (2008)). Although such a cyclic traffic flow has an uncontrollable zero eigenvalue themselves, in this paper, we show that the cyclic traffic flow is controllable. In addition, we apply washout control which can stabilize traffic flow and show that washout control is useful to suppress the traffic jam.

This paper is organized as follows. Section 2 explains the optimal velocity model and its dynamics. In addition, we derive a linearized system of the optimal velocity model for analyzing the control systems. In Section 3, we describe washout control which is applied to the suppression of the traffic jam. In Section 4, we briefly review a small gain stability condition in terms of parameters of washout controller. In Section 5, we derive another stability condition of the closed-loop system together with showing that the A-matrix of the closed-loop system necessarily has a zero eigenvalue, and its right eigenvector is restricted to be a zero vector. In Section 6, by comparing the proposed method with a previous small gain based method, our proposed method is more useful to suppress the traffic jam in a cyclic traffic flow. Finally, conclusions are presented in Section 7.

2. OPTIMAL VELOCITY MODEL

We consider N vehicles run on a circle with radius r in a counterclockwise direction (Fig. 1). We denote the phase angle of the ith vehicle by $\theta_i(t)$. And we denote the relative angle between $(i-1)$th and ith vehicles by $\varphi_i(t)$, which described as

$$\varphi_i(t) = \theta_{i-1}(t) - \theta_i(t),$$

where

$$\varphi_1(t) = \theta_N(t) - \theta_1(t) + 2\pi.$$

In addition, we denote the $y_i(t)$ is the headway distance between $(i-1)$th and ith vehicles, which described as

$$y_i(t) = r\varphi_i(t).$$

All vehicles are modeled as

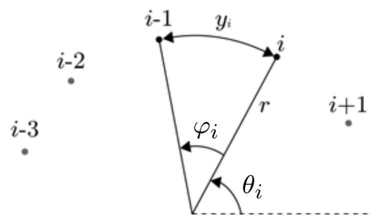

Fig. 1. A cyclic traffic flow model.

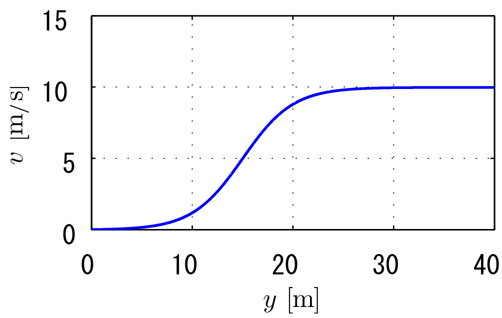

Fig. 2. The optimal velocity function $v = F(y)$ which is used in this paper ($b = 5$, $c = 5$, $y^* = 15$)

$$\begin{cases} \dot{v}_i(t) = a\{F(y_i(t)) - v_i(t)\} + u_i(t) \\ \dot{y}_i(t) = v_{i-1}(t) - v_i(t), \end{cases} \tag{1}$$

where $v_i(t)$ is the velocity of ith vehicles, a is the sensitivity of a driver, $u_i(t)$ is the control input. The optimal velocity function $F(y_i(t))$ is assumed to be described as

$$F(y_i(t)) = b\left\{\tanh\left(\frac{y_i(t) - y^*}{c}\right) + \tanh\left(\frac{y^*}{c}\right)\right\}, \tag{2}$$

where b, c, and y^* are parameters which we tune the optimal velocity. This function is illustrated in Fig. 2. It is also assumed that when all vehicles run with $u \equiv 0$, (1) has an equilibrium state

$$[v_i^* \ y_i^*] = \left[b\tanh\left(\frac{y^*}{c}\right) \ y^*\right]. \tag{3}$$

Defining small deviations from the equilibrium as

$$\bar{v}_i(t) := v_i(t) - v_i^*,$$
$$\bar{y}_i(t) := y_i(t) - y_i^*,$$

we obtain the linearized dynamics of the vehicle system (1) around the equilibrium state (3) as

$$\begin{cases} \dot{\bar{v}}_i(t) = a\{\Lambda\bar{y}_i(t) - \bar{v}_i(t)\} + u_i(t) \\ \dot{\bar{y}}_i(t) = \bar{v}_{i-1}(t) - \bar{v}_i(t), \end{cases}$$

where

$$\Lambda := \left.\frac{\partial F(y)}{\partial y}\right|_{y=y^*}$$

is the first derivative of the optimal velocity function at $y = y^*$. Here, note that the sum of the headway distance is equal to the circumference in a cyclic traffic flow, i.e.,

$$\sum_{i=1}^{N} y_i^* = 2\pi r. \tag{4}$$

In addition, from (4) we can derive following constraint conditions

$$\sum_{i=1}^{N} y_i(t) = 2\pi r,$$
$$\sum_{i=1}^{N} \{\bar{y}_i(t) + y_i^*\} = 2\pi r,$$
$$\sum_{i=1}^{N} \bar{y}_i(t) = 0. \tag{5}$$

By choosing the state vector as

$$\bar{w}_i = \begin{bmatrix} \bar{v}_i(t) \\ \bar{y}_i(t) \end{bmatrix},$$

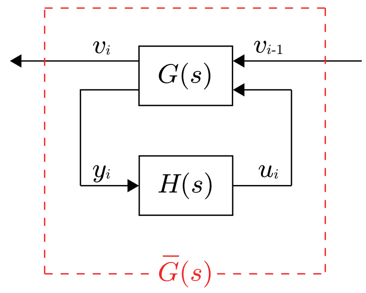

Fig. 3. The ith controlled vehicle with the washout controller $H(s)$.

a state space realization is given by

$$\begin{cases} \dot{\bar{w}}_i = \begin{bmatrix} -a & a\Lambda \\ -1 & 0 \end{bmatrix} \bar{w}_i + \begin{bmatrix} 0 \\ 1 \end{bmatrix} \bar{v}_{i-1} + \begin{bmatrix} 1 \\ 0 \end{bmatrix} \bar{u}_i \\ \bar{v}_i = [1 \ 0]\, \bar{w}_i \\ \bar{y}_i = [0 \ 1]\, \bar{w}_i. \end{cases} \tag{6}$$

From (6), we can derive the transfer function $G(s)$ from $\begin{bmatrix} \bar{v}_{i-1}(t) \\ \bar{u}_i(t) \end{bmatrix}$ to $\begin{bmatrix} \bar{v}_i(t) \\ \bar{y}_i(t) \end{bmatrix}$ as

$$G(s) = \frac{1}{s^2 + as + a\Lambda} \begin{bmatrix} a\Lambda & s \\ s + a & -1 \end{bmatrix}. \tag{7}$$

3. WASHOUT CONTROL

In the optimal velocity traffic model, driver's intention is expressed by $F(y)$. In general, it is difficult to exactly describe it. Hence, there exists uncertainty in $F(y)$ and y^*. Furthermore, v_i^* and y_i^* may be different from driver's intention. If we use v_i^* and y_i^* as a reference input to stabilize the system, it would be inconsistent with driver's intention. It is known that washout control can stabilize the equilibrium point without using it as a reference input (Takimoto, Yamamoto, and Oku (2008)). A washout controller for the ith vehicle is given by

$$\begin{cases} \dot{\xi}_i(t) = \alpha\xi_i(t) + \beta y_i(t) \\ u_i(t) = \alpha\xi_i(t) + \beta y_i(t) \end{cases}. \tag{8}$$

where parameters α and β are chosen to suppress the traffic jam. Then, we can derive the transfer function $H(s)$ from $y_i(t)$ to $u_i(t)$ as

$$H(s) = \alpha(s - \alpha)^{-1}\beta + \beta = \frac{\beta s}{s - \alpha}.$$

When we use (8) for (7), we have the transfer function $\bar{G}(s)$ from $\bar{v}_{i-1}$ to $\bar{v}_i$ as

$$\bar{G}(s) = \frac{(a\Lambda + \beta)s - a\Lambda\alpha}{s^3 + (a - \alpha)s^2 + (a\Lambda + \beta - a\alpha)s - a\Lambda\alpha},$$
$$= \frac{n_1 s + n_2}{s^3 + d_1 s^2 + d_2 s + d_3},$$

where

$$d_1 = a - \alpha,$$
$$d_2 = a\Lambda + \beta - a\alpha,$$
$$d_3 = -a\Lambda\alpha,$$
$$n_1 = a\Lambda + \beta,$$
$$n_2 = d_3.$$

Fig. 3 represents the block diagram of the ith controlled vehicle with a washout controller (8).

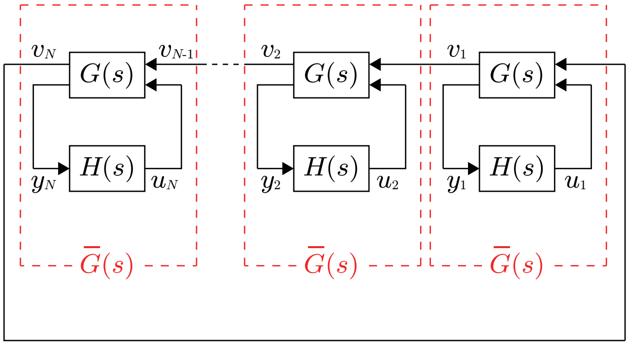

Fig. 4. The closed-loop system.

4. SMALL GAIN CONDITION

Then, the region Ω_1 for parameters α and β such that $\bar{G}(s)$ is stable can be derived as

$$\Omega_1 := \{(\alpha,\ \beta)|\ \alpha < 0,\ d_2 > 0,\ d_1 d_2 - d_3 > 0\}$$

by using the Routh stability criterion. Here, Fig. 4 shows that the closed-loop system. The velocity $\bar{v}_i$ is described as

$$v_i = \left\{\bar{G}(s)\right\}^N v_i.$$

Hence, if $\|\bar{G}(s)\|_\infty \leq 1$, the velocity $\bar{v}_i$ cannot diverge from the velocity of equilibrium state v_i^* even if the number of vehicles increases. Additionally, the region Ω_2 for parameters α and β such that $\|\bar{G}(s)\|_\infty \leq 1$ is derived as

$$\Omega_2 := A \cap (B \cup C \cup D),$$

where

$$\begin{aligned}
A &= \{(\alpha,\ \beta)|\ \zeta > 0\},\\
B &= \{(\alpha,\ \beta)|\ \eta > 0\},\\
C &= \left\{(\alpha,\ \beta)|\ \eta^2 - 4\zeta < 0\right\},\\
D &= \left\{(\alpha,\ \beta)|\ \eta^2 - 3\zeta < 0\right\},\\
\zeta &= {d_2}^2 - 2d_1 d_3 - {n_2}^2,\\
\eta &= {d_1}^2 - 2d_2.
\end{aligned}$$

Hence, the intersection $\Omega_1 \cap \Omega_2$ where gives parameters suppressing traffic jam is illustrated as in Fig. 5. We used parameters $a = 1.0$ and $\Lambda = 1.0$ to draw Fig. 5.

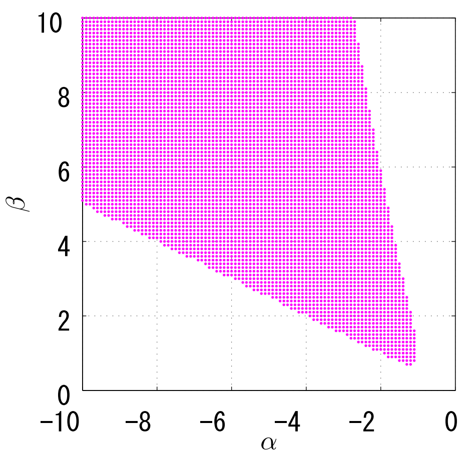

Fig. 5. The region $\Omega_1 \cap \Omega_2$ of the controller parameters α and β.

5. DETAILED ANALYSIS OF THE CLOSED-LOOP

When each vehicle is controlled by the washout controller, the closed-loop system can be described as

$$\dot{x} = Ax, \tag{9}$$

where

$$x = \begin{bmatrix} x_1 \\ \vdots \\ x_N \end{bmatrix} \in \mathbb{R}^{3N},\ x_i = \begin{bmatrix} \bar{v}_i \\ \bar{y}_i \\ \bar{\xi}_i \end{bmatrix} \in \mathbb{R}^3, \tag{10}$$

$$A = \begin{bmatrix} A^* & 0 & \cdots & 0 & B^* \\ B^* & A^* & 0 & \cdots & 0 \\ 0 & \ddots & \ddots & \ddots & \vdots \\ \vdots & \ddots & \ddots & \ddots & 0 \\ 0 & \cdots & 0 & B^* & A^* \end{bmatrix} \in \mathbb{R}^{3N \times 3N}, \tag{11}$$

$$A^* = \begin{bmatrix} -a & a\Lambda + \beta & \alpha \\ -1 & 0 & 0 \\ 0 & \beta & \alpha \end{bmatrix},\ B^* = \begin{bmatrix} 0 & 0 & 0 \\ 1 & 0 & 0 \\ 0 & 0 & 0 \end{bmatrix}. \tag{12}$$

Theorem 1. The eigenvalues of (11) are roots of

$$D(s)^N - S_{12}(s)^N, \tag{13}$$

where

$$\begin{aligned}
D(s) &= s^3 + (a - \alpha)s^2 + (a\Lambda + \beta - a\alpha)s - a\Lambda\alpha,\\
S_{12}(s) &= (a\Lambda + \beta)s - a\Lambda\alpha.
\end{aligned}$$

Proof.

$$\begin{aligned}
&|sI - A| \\
&= \begin{vmatrix} sI - A^* & 0 & \cdots & 0 & -B^* \\ -B^* & sI - A^* & 0 & \cdots & 0 \\ 0 & \ddots & \ddots & \ddots & \vdots \\ \vdots & \ddots & \ddots & \ddots & 0 \\ 0 & \cdots & 0 & -B^* & sI - A^* \end{vmatrix} \\
&= |sI - A^*| \left| \begin{bmatrix} sI - A^* & 0 & \cdots & 0 \\ -B^* & \ddots & \ddots & \vdots \\ & \ddots & \ddots & 0 \\ 0 & & -B^* & sI - A^* \end{bmatrix} \right. \\
&\qquad \left. - \begin{bmatrix} -B^* \\ 0 \\ \vdots \\ 0 \end{bmatrix} (sI - A^*)^{-1} \begin{bmatrix} 0 & \cdots & 0 & -B^* \end{bmatrix} \right| \\
&= |sI - A^*|^{N-1} \\
&\quad \times \left| (sI - A^*) - \left\{ B^* (sI - A^*)^{-1} \right\}^{N-1} B^* \right| \\
&= |sI - A^*|^N \\
&\quad \times \left| I - (sI - A^*)^{-1} \left\{ B^* (sI - A^*)^{-1} \right\}^{N-1} B^* \right| \\
&= |sI - A^*|^N \left| I - \left\{ (sI - A^*)^{-1} B^* \right\}^N \right|
\end{aligned} \tag{14}$$

where

$$(sI - A^*)^{-1} = \frac{1}{D(s)} \begin{bmatrix} S_{11}(s) & S_{12}(s) & S_{13}(s) \\ S_{21}(s) & S_{22}(s) & S_{23}(s) \\ S_{31}(s) & S_{32}(s) & S_{33}(s) \end{bmatrix}$$

$$
\begin{aligned}
S_{11}(s) &= s(s-\alpha),\\
S_{12}(s) &= (a\Lambda+\beta)s - a\Lambda\alpha,\\
S_{13}(s) &= \alpha s,\\
S_{21}(s) &= -(s-\alpha),\\
S_{22}(s) &= s-\alpha,\\
S_{23}(s) &= -\alpha,\\
S_{31}(s) &= -\beta,\\
S_{32}(s) &= \beta(s+a),\\
S_{33}(s) &= s(s+a) + (a\Lambda+\beta).
\end{aligned}
$$

Furthermore, a determinant calculation from (14) to (15) is shown as follows.

$$
\begin{aligned}
&\left| I - \left\{ (sI - A^*)^{-1} B^* \right\}^N \right| \\
&= \left| I - \left\{ \frac{1}{D(s)} \begin{bmatrix} S_{11}(s) & S_{12}(s) & S_{13}(s) \\ S_{21}(s) & S_{22}(s) & S_{23}(s) \\ S_{31}(s) & S_{32}(s) & S_{33}(s) \end{bmatrix} \begin{bmatrix} 0 & 0 & 0 \\ 1 & 0 & 0 \\ 0 & 0 & 0 \end{bmatrix} \right\}^N \right| \\
&= \left| I - \left\{ \frac{1}{D(s)} \begin{bmatrix} S_{12}(s) & 0 & 0 \\ S_{22}(s) & 0 & 0 \\ S_{32}(s) & 0 & 0 \end{bmatrix} \right\}^N \right| \\
&= \left| I - \frac{1}{D(s)^N} \begin{bmatrix} S_{12}(s)^N & 0 & 0 \\ S_{22}(s)S_{12}(s)^{N-1} & 0 & 0 \\ S_{32}(s)S_{12}(s)^{N-1} & 0 & 0 \end{bmatrix} \right| \\
&= \begin{vmatrix} 1 - \left\{ \dfrac{S_{12}(s)}{D(s)} \right\}^N & 0 & 0 \\ -\dfrac{S_{22}(s)S_{12}(s)^{N-1}}{D(s)^N} & 1 & 0 \\ -\dfrac{S_{32}(s)S_{12}(s)^{N-1}}{D(s)^N} & 0 & 1 \end{vmatrix}.
\end{aligned}
$$

Thus,

$$
\begin{aligned}
|sI - A| &= |sI - A^*|^N \begin{vmatrix} 1 - \left\{ \dfrac{S_{12}(s)}{D(s)} \right\}^N & 0 & 0 \\ -\dfrac{S_{22}(s)S_{12}(s)^{N-1}}{D(s)^N} & 1 & 0 \\ -\dfrac{S_{32}(s)S_{12}(s)^{N-1}}{D(s)^N} & 0 & 1 \end{vmatrix} \qquad (15)\\
&= |sI - A^*|^N \left[1 - \left\{ \frac{S_{12}(s)}{D(s)} \right\}^N \right] \\
&= D(s)^N - S_{12}(s)^N.
\end{aligned}
$$

□

Corollary 2. The system (9) necessarily has one zero eigenvalue. In addition, the right eigenvector associated with the zero eigenvalue is a zero vector.

Proof. Assigning (13) to $s = 0$,

$$D(0)^N - S_{12}(0)^N = (-a\Lambda\alpha)^N - (-a\Lambda\alpha)^N = 0.$$

Hence, the A-matrix has at least one zero eigenvalue. A right eigenvector associated with the zero eigenvalue of the A-matrix is described as

$$
\bar{x}_R = \begin{bmatrix} \bar{x}_r \\ \vdots \\ \bar{x}_r \end{bmatrix} \in \mathbb{R}^{3N},\ \bar{x}_r = \begin{bmatrix} -\Lambda\alpha\gamma \\ -\alpha\gamma \\ \beta\gamma \end{bmatrix} \in \mathbb{R}^3 \quad (\gamma \text{ is const.}). \qquad (16)
$$

i.e., when $x = \bar{x}_R$, $\dot{x} = 0$. Hence, from (10) and (16)

$$\sum_{i=1}^{N} \bar{y}_i = -\alpha N \gamma. \qquad (17)$$

However, it follows from the constraint condition (5) that $\gamma = 0$. Hence, when $\dot{x} = 0$, the state x must be

$$x = 0.$$

□

In general, when the A-matrix has at least one zero eigenvalue, the system is unstable. However, a right eigenvector associated with the zero eigenvalue of the A-matrix implies an equilibrium state from Corollary 2, because a cyclic traffic flow has the constraint condition (5). Thus, it is sufficient for the closed-loop system (9) to be stable that all A-matrix's eigenvalues except for zero eigenvalues are stable. Next corollary gives us a condition of parameters α and β such that the closed-loop system is stable.

Corollary 3. Parameters α and β such that the eigenvalues of the A-matrix of the closed-loop system are stable can be determined by the following polynomials.

(i) When N is odd ($N = 2n + 1$),

$$F_o(s) = \prod_{i=1}^{n} V_i(s).$$

(ii) When N is even ($N = 2n$),

$$F_e(s) = (D(s) + S_{12}(s)) \prod_{i=1}^{n-1} V_i(s),$$

where

$$V_i(s) = D(s)^2 - 2D(s)S_{12}(s)\cos\left(\frac{2\pi}{N} i\right) + S_{12}(s)^2.$$

Proof. When we factorize (13), we have to consider whether the number of vehicle N is odd or even. When $N = 2n + 1$,

$$D(s)^{2n+1} - S_{12}(s)^{2n+1} = (D(s) - S_{12}(s))\, F_o(s).$$

On the other hand, when $N = 2n$,

$$D(s)^{2n} - S_{12}(s)^{2n} = (D(s) - S_{12}(s))\, F_e(s).$$

□

The region of parameters α and β for closed-loop stability can be shown in Fig. 6 and Fig. 7. To draw them, we used parameters $a = 1.0$ and $\Lambda = 1.0$.

6. COMPARISON WITH A PREVIOUS METHOD

When $N = 20$, we compare the region for parameters α and β such that the closed-loop system is stable (Fig. 7) with the region $\Omega_1 \cap \Omega_2$ (Fig. 5) and the result is illustrated in Fig. 8. Fig. 8 is a superimposed figure Fig. 5 on Fig. 7. Fig. 9, Fig. 10 and Fig. 11 are close-ups of Fig. 8. Red circles show the parameters α and β which form the region $\Omega_1 \cap \Omega_2$. Green christcrosses show the parameters α and β which imply the region such that closed-loop system is stable at $N = 20$. It can be seen from Fig. 9, Fig. 10 and Fig. 11 that the region is expanded.

Fig. 12 and Fig. 13 are the space-time plots of the distance $y_1(t) - y_i(t)$ from $t = 100$ to 300 for all vehicles using the

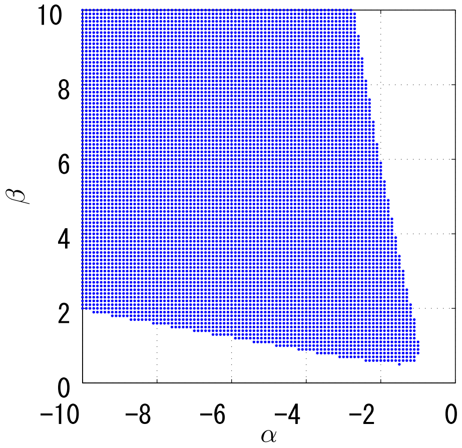

Fig. 6. Stability region when the number of vehicles $N = 6$.

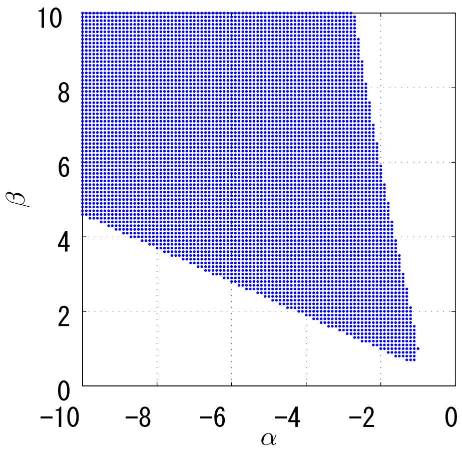

Fig. 7. Stability region when the number of vehicles $N = 20$.

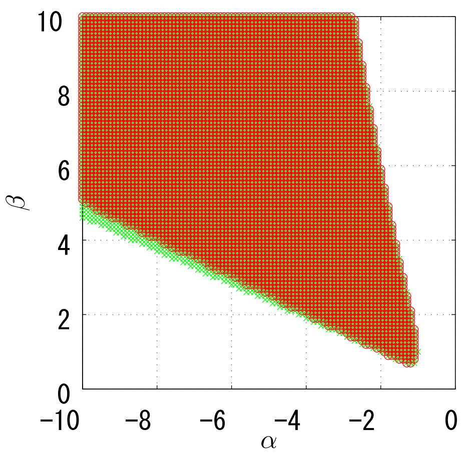

Fig. 8. A comparison of Fig. 5 and Fig. 7.

parameters α and β which we select from the expanded stability region. We find no traffic jam in the simulation from Fig. 12 and Fig. 13. Hence, by comparing with the previous method based on the small gain theorem, the proposed method is more useful to suppress the traffic jam in the cyclic traffic flow.

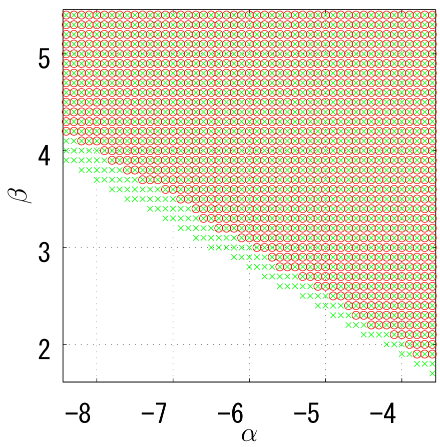

Fig. 9. Close-up of the left lower area of Fig. 8.

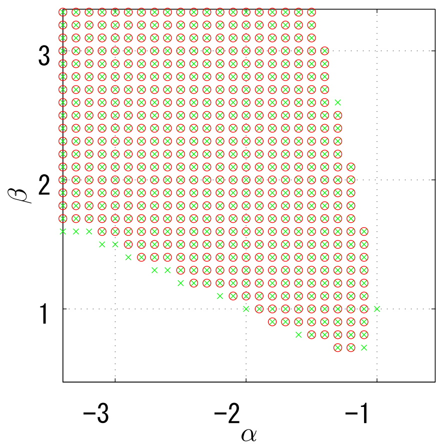

Fig. 10. Close-up of the right lower area of Fig. 8.

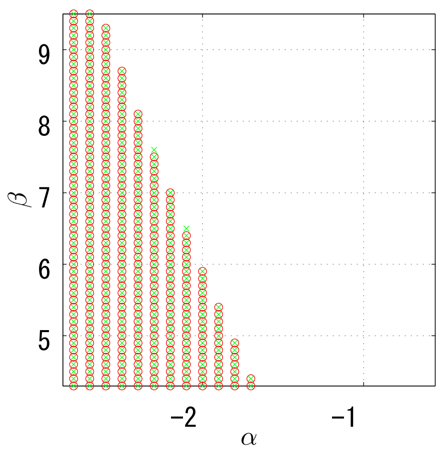

Fig. 11. Close-up of the right upper area of Fig. 8.

7. CONCLUSION

In this paper, we applied washout control to suppress the traffic jam in the cyclic traffic flow. In addition, we showed that the numerical simulations which illustrate the effectiveness of the proposed method. By comparing the proposed method with a conservative method based on the

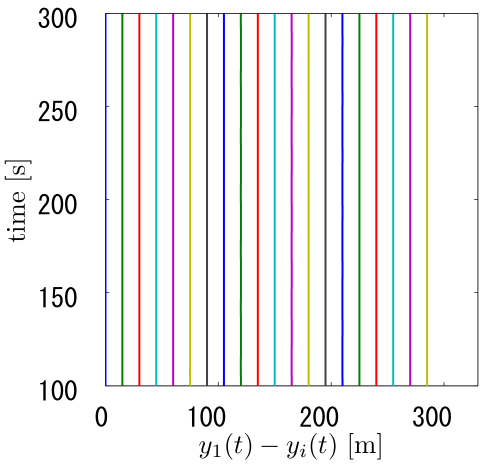

Fig. 12. Space-time plot by using control with $\alpha = -8$ and $\beta = 4$.

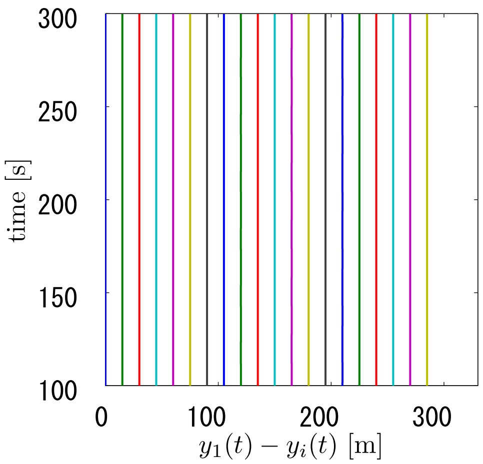

Fig. 13. Space-time plot by using control with $\alpha = -4$ and $\beta = 2$.

small gain theorem, it is realized that we obtain a much precise stability region.

REFERENCES

Bando, M. *et al.* (1995). Dynamical model of traffic congestion and numerical simulation. *Physical Review E*, vol. 51, no. 2, pp. 1035–1042.

Eyne, J., Yanakiev, D. and Kanellakopoulos, I. (1998). A Simplified Framework for String Stability Analysis of Automated Vehicle System Dynamics. *Vehicle System Dynamics*, vol. 30, no. 5, pp. 375–405.

Khaisongkram, W. and Hara, S. (2010). Performance Analysis of Decentralized Cooperative Driving under Non-symmetric Bidirectional Information Architecture. *IEEE International Conference on Control Applications*, pp. 2035–2040.

Konishi, K., Kokame, H., and K. Hirata, (2000). Decentralized delayed-feedback control of an optimal velocity traffic model. *The European Physical Journal B*, vol. 15, pp. 715–722.

Seiler, P., Pant, A. and Heddrick, K. (2004). Disturbance Propagation in Vehicle Strings. *IEEE Transactions on Automatic Control*, vol. 49, no. 10, pp. 1835–1841.

Sugiyama, Y. *et al.* (2008). Traffic jams without bottlenecks – experimental evidence for the physical mechanism of the formation of a jam. *New Journal of Physics 10*, 033001.

Takimoto, T., Yamamoto, S. and Oku, H. (2008). Washout Control for Manual Operations. *IEEE Transactions on Control Systems Technology*, vol. 16, no. 6, pp. 1169–1176.

Yamamoto, S. and Sakaguchi, E. (2009). Driver Centric Decentralized Controller Design in Traffic Flow. *ICCAS–SICE 2009*, pp. 246–250.

Yang, Y. and Tongue, B. (1996). A New Control Approach for Platoon Operations during Vehicle Exit/Entry. *Vehicle System Dynamics*, vol. 25, no. 4, pp. 305–319.

Zhang, Y. *et al.* (1999). Autonomous Intelligent Cruise Control Using Front and Back Information for Tight Vehicle Following Maneuvers. *IEEE Transactions on Vehicular Technology*, vol. 48, no. 1, pp. 319–328.